

# Rotating Curvilinear Tools for EDM of Polygonal Shapes with Sharp Corners

[CIRP Annals 56 \(2007\) 221-224](#)

Y. Ziada, P. Koshy (2)

Department of Mechanical Engineering, McMaster University, Hamilton, Canada

## Abstract

Flushing of the inter-electrode gap is of critical importance in the performance of electrical discharge sinking operations. When the provision of flushing holes in the tool or the workpiece is impractical, effective flushing is best realized by inducing a relative motion between the electrodes. This paper relates to a novel application inspired by the kinematics of a Reuleaux Triangle that facilitates flushing through synchronous orbiting of a rotating curvilinear tool. This innovative scheme enables the machining of regular as well as non-regular polygonal shapes with sharp corners. Experimental results from implementing this concept on a 4-axis CNC EDM machine tool are presented.

## Keywords:

Electrical discharge machining (EDM), Kinematic, Reuleaux Triangle

## 1 INTRODUCTION

Material removal in electrical discharge machining (EDM) entails the generation of debris in the working gap that comprises eroded electrode particles and by-products of dielectric decomposition [1]. Uniformly distributed gap contamination of a certain threshold is desirable in the interest of discharge initiation; however, excessive debris concentration confined to isolated domains in the gap due to insufficient flushing leads to repeated localization of the discharge location. This has unfavourable ramifications on process stability, and the geometry and integrity of the machined surface. Adequate gap flushing is therefore decisive in terms of both machining productivity and the quality of the machined surface.

Flushing could be accomplished by forced flow of the dielectric fluid through holes in the tool, but flushing holes leave their footprints on the machined surface, as the work shape generated in EDM is complementary to that of the tool. Flushing could alternatively be through micro-holes specially fabricated in the tool [2]. In the instance that it is infeasible to provide flushing holes in either of the electrodes, the dielectric could be directed at the gap in the form of a jet from outside the machining zone. This technique is not effective when the machined depth or the frontal machining area is large: conditions that pertain to an acute need for good flushing.

Another approach to flushing is to introduce a secondary motion between the tool and the workpiece. In the jump-EDM process, the tool is periodically retracted off the gap to allow for the removal of the contaminated dielectric. Tool motion can further be extended to more than one axis [3], in which case the tool and the workpiece essentially constitute a pump that constantly regenerates the gap. These techniques are limited by the additional tool movement representing lost machining time.

Other techniques that invoke a relative motion between the tool and the workpiece include planetary EDM [4-6], which involves a lateral translation of the tool that is geometrically similar to the machined shape, and processes that employ rotating disk-shaped tools. The introduction of computer numerically controlled (CNC) sinkers of late have spurred electrical discharge milling technology [7], which employs rotating tools of a simple cylindrical shape that follow a programmed path to machine a cavity, similar to end-milling operations. Rotating tools are beneficial in terms of inducing flushing

and evenly distributing tool wear, but they rule out the machining of sharp corners. Fine features could be generated with rotating tools of an appropriate radius, but their application is not productive as the limited engagement restricts the maximum machining power, and hence the removal rate.

In this context, the present work relates to the design and implementation of novel tool kinematics motivated by the concept of a Reuleaux Triangle (RT). The technique utilizes rotating curvilinear tools for sinking regular and non-regular polygonal cavities with sharp corners, with a view to enhancing gap flushing while concurrently maximizing the frontal machining area. The work is a step towards exploiting the capability of modern multi-axis CNC ram EDM. The concept can also enhance electrochemical machining performance [8].

## 2 EDM WITH REULEAUX TRIANGLE TOOLS

The concept of using rotating RT tools is introduced in this section by first considering EDM of a square cavity with rounded corners. The idea is subsequently extended to a square cavity with sharp corners, as well as regular and non-regular polygons.

To machine a square cavity using a rotating tool, it is essential that the tool shape can be inscribed and turned within the cavity without restraint, such that the tool sweeps the shape without crossing its boundary. This constrains the tool to be preferably of a shape of constant width, which means that the distance between two opposing parallel lines tangent to its profile is constant for all orientations. A circle is a shape of constant width, but a tool of a circular section is not of interest from the viewpoint of being able to machine sharp corners. The RT named after Franz Reuleaux who seems to have first discussed it in the context of theory of machines [9], is the simplest non-circular shape of constant width and is of particular interest in this regard.

The kinematics of a RT, which is rather counterintuitive, can be elucidated with the aid of Figure 1. The construction of a RT involves the frame of an equilateral triangle 123 of side length  $s$ , the sides of which are replaced by circular arcs 12, 23 and 31 of identical radius  $s$  that are centered on vertices 3, 1 and 2, respectively. The RT can rotate inside a square, and as it rotates clockwise such that vertex 1 traverses the first quadrant,

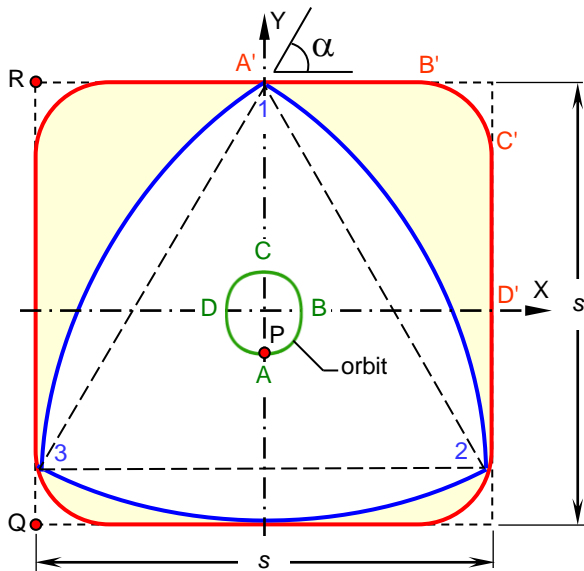


Figure 1: Elements of RT kinematics.

it traces the path  $A'B'C'D'$ . Segments  $A'B'$  and  $C'D'$  are linear while segment  $B'C'$  is part of an ellipse with its major axis oriented at  $45^\circ$  to the X-axis and centered at point Q in the third quadrant.

For the position of the RT shown in Figure 1, its centroid P is located at A. The clockwise motion of vertex 1 along  $A'B'$ ,  $B'C'$  and  $C'D'$  corresponds to the counter clockwise motion of P along AB, BC and CD, respectively. Each of these segments that constitute the orbit is part of an ellipse; for instance, path AB is part of an ellipse with its major axis oriented at  $135^\circ$  to the X-axis and centered at point R in the fourth quadrant. Path AB of centroid P is defined by the parametric equations:

$$x_P = \frac{s}{6} (-3 + \sqrt{3} \cos \alpha + 3 \sin \alpha) \quad (1)$$

$$y_P = \frac{s}{6} (3 - 3 \cos \alpha - \sqrt{3} \sin \alpha) \quad (2)$$

where  $\alpha$  is the angle between the side of the equilateral triangle and the linear segment traced (say  $31$  and  $A'B'$ ), which varies from  $60^\circ$  to  $30^\circ$  as P moves from A to B, corresponding to vertex 1 translating from  $A'$  to  $B'$ . Segments BC and CD of the orbit can be obtained by symmetry. For every complete rotation of the RT inside the square, its centroid therefore orbits thrice in the opposite direction. Equations (1) and (2) imply that the orbit is bounded by a square of side  $0.16s$ . Additional mathematical details and an animation can be found in Reference [9].

Although the shape swept does not have sharp corners, the RT which has a frontal area that is 70.5% of the square, sweeps 98.8% of the square [9]. To put this in perspective, if a similar corner were to be machined using a cylindrical tool, the corresponding frontal area would be only about 4%. For machining applications wherein such rounded corners are unacceptable, a method that generates sharp corners is presented in the next section.

The rotating RT must be synchronously translated along the geometrically complex orbit such that a ratio of 1:3 is maintained between the rotational and translational components of tool motion, otherwise the intended square shape would degenerate into a circle. This necessitates a 4-axis CNC EDM for implementation. The rotational speed of the RT tool is further constrained by the maximum feed speed of the machine tool X/Y axes that currently is rather low, typically less than

1.5 m/min on modern CNC ram EDM with ball screw drives.

Graphical simulations indicate that an approximation of the composite orbit by a circle of diameter  $0.16s$  corresponds to a maximum deviation of just  $0.003s$  in respect of the profile obtained. For applications where such a small deviation is of no consequence, a simple fixture that involves a planetary gear train could be used to execute this scheme on a conventional machine tool with one servo controlled axis. This also enables the use of higher tool rotational speeds, as it is independent of and not limited by the feed speed of the machine tool X/Y axes. Experimental results that compare the performance of a RT tool from such a set-up with that of a conventional stationary tool in the machining of aluminum ( $s = 86$  mm) using a copper tool with positive polarity are presented in Figure 2a. It is evident that due to the improved flushing the removal rate is manyfold higher and is maintained independent of the machining time in the case of the RT tool, in stark contrast to the stationary tool. The latter was further found to sustain severe arcing that adversely affected the integrity of the machined surface (Figure 2b), while the surface machined by the RT tool was free of such (Figure 2c).

RT tools can significantly improve productivity in EDM due to enhanced gap flushing induced by tool rotation and translation. Flushing can further be augmented in this process by means of external jet flushing, as the RT only partially covers the square at any instant, which leaves ample peripheral clearance for the ingress and egress of the dielectric fluid. Although rotation of the tool is in general associated with beneficially distributing tool wear over a larger area, the tool motion [3] and the adverse current density distribution render the vertices of the RT tool susceptible to rapid wear leading to deviations from the intended profile. As in conventional EDM practice, such errors can be corrected for by using a finishing tool or by periodically truing the worn tool.

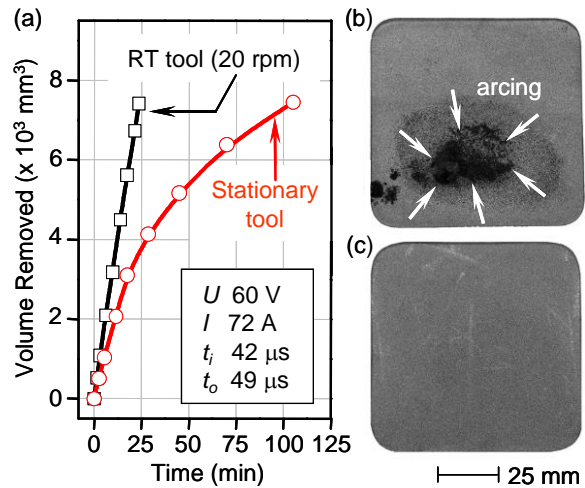


Figure 2: Performance of RT and conventional tools.

### 3 EDM OF A SQUARE WITH SHARP CORNERS

The RT has found applications in the modern Wankel engine and a mechanical drill for machining square holes with round corners (US patent 1,241,175 of 1917). The innovative aspect of the present work is its application in EDM, and more significantly, its extension to EDM of shapes with sharp corners.

As the vertex of a RT subtends an angle of  $120^\circ$ , it cannot be used as such to machine square shapes with sharp corners, and hence calls for a geometric modification. Similar to the RT, the modified shape comprises three

circular arcs (Figure 3) that replace the sides of an equilateral triangle of side  $s$ , but the arcs are of radius  $ks$  rather than  $s$  in the case of the RT, where  $k$  is a constant that works out to be 1.93 for the included angle to be  $90^\circ$ . This is not a shape of constant width but can rotate within a square and generate sharp corners. The area of the modified RT is 57.8% of the square.

As in the discussion on machining of a square with

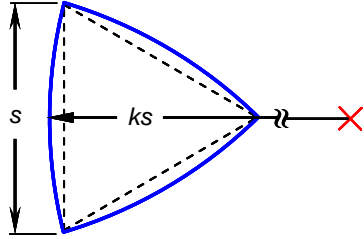


Figure 3: Construction of a modified RT.

rounded corners in Section 2, the generation of a square with sharp corners is explained in the following with reference to the first quadrant. Figure 4a shows the initial (emphasised) and several successive positions of the modified RT as its centroid  $P$  traverses the path  $ABC$ . Segment  $AB$  is defined by Equations (1) and (2) for angle  $\alpha$  (as defined in Figure 1) varying between  $60^\circ$  and  $15^\circ$ , as opposed to between  $60^\circ$  and  $30^\circ$  in the case of a square with rounded corners. Segment  $BC$  of the centroidal path is obtained by symmetry about line  $BB'$ . Linear segments  $A'B'$  and  $B'C'$  on the generated profile correspond to the paths  $AB$  and  $BC$ , respectively.

Figure 4a indicates that the generated envelope oversteps the intended square of side  $s$  at the top left corner in the fourth quadrant, and stops short of it in the first quadrant by  $0.034s$  along both the  $X$  and  $Y$  axes at points  $B'$  and  $C'$ , respectively. These deviations can be corrected by altering the  $x$ -component of the centroidal path along  $AB$  as:

$$x_p = \frac{s}{6}(-3 + \sqrt{3} \cos \alpha + 3 \sin \alpha) + \beta s \left( \frac{60 - \alpha}{180/n} \right) \quad (3)$$

which is essentially the same as Equation (1) but for the additional term that refers to the correction of  $\beta s$  applied linearly in a scale of 0 to 1 as  $\alpha$  varies from  $60^\circ$  to  $15^\circ$ ; in this case,  $\beta$  is 0.034 and  $n$  (the number of sides of the polygon) is equal to 4. No such correction is required for the  $y$ -component per se, as path  $BC$  is obtained by symmetry. The envelope corresponding to the corrected orbit is shown in Figure 4b, which indicates that indeed a part of the required square with a sharp corner is generated in the first quadrant, and that the envelope of

tool positions is contained within the intended square. Iterating this motion four times over a path appropriately obtained by symmetry completes the entire square. Such an orbit is complex and requires a 4-axis CNC machine tool.

Figure 4c depicts a square cavity with sharp corners machined using this scheme as a proof of concept. A comparison of the performance of the RT tool with that of a conventional stationary tool could not be realized on account of the tool rotational speed being severely limited by the low  $X/Y$  axes feed speeds, as indicated previously. As can be seen in Figure 4b which emphasises the position of the modified RT at the instant it generates the corner  $B'$ , only one of the tool vertices is engaged in the machining of the corner. This vertex is hence selectively subject to additional wear, which has a negative influence on the corner generation accuracy. This further leaves striations on the machined surface along the profile as can be observed in the photograph of the machined cavity. The issue of additional wear in one of the tool vertices could be circumvented somewhat by periodically indexing the tool through  $120^\circ$  so as to distribute the wear evenly between the three vertices of the tool. The tool tips could also be of a material that is more resistant to spark erosion.

#### 4 EDM OF REGULAR POLYGONS

The concepts presented in Sections 2 and 3 form the basis for the EDM of polygonal shapes using rotating curvilinear tools. As the included angle of the RT is  $120^\circ$  it can be used as such for machining polygons with number of sides exceeding 5. For machining a pentagon, the included angle at the tool tip has to be  $108^\circ$ , which is accomplished as indicated in Figure 3, for  $k$  assuming a value of 1.23. Machining of a triangular shape is possible but not considered in this paper.

For the machining of polygons, the tool size is determined by the largest equilateral triangle that can be rotated within the polygon. It is expedient to realise this through recursive geometric modelling. Tool size  $s$  determined thus is presented in Table 1, as a function of the number of sides of the polygon  $n$  and its side length  $d$ . The use of rotating tools based on the RT are rendered less effective as the number of sides of the polygon increases, on account of the reduction in tool frontal area in respect of the machined area.

The extension of the principle of a RT to machining polygonal shapes is quite straightforward and is perhaps best explained with reference to a hexagon as an example. This is indicated in Figure 5a wherein the centroidal path is enlarged (3X) for clarity, and segments of the centroidal path are shown colour matched with the

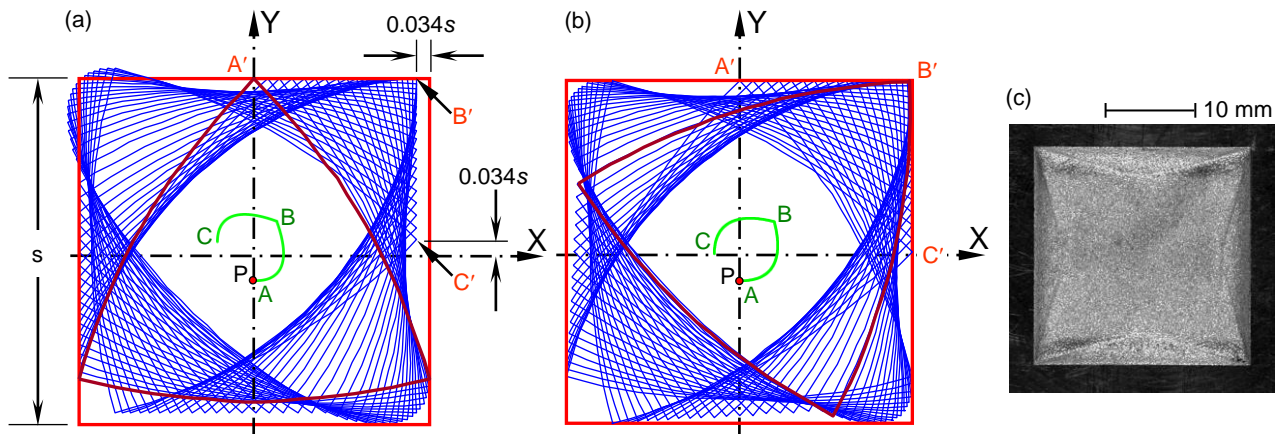


Figure 4: Generation of a square with a sharp corner using a modified RT.

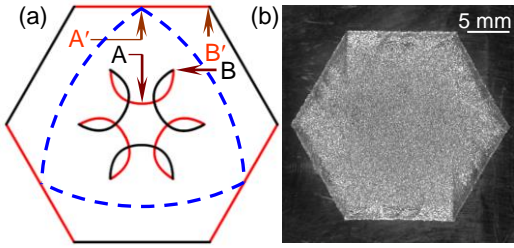


Figure 5: Machining of a hexagonal cavity.

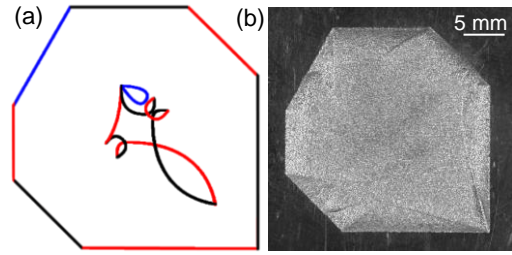


Figure 6: Machining of a non-regular cavity.

respective generated sides of the polygon. The initial position of the RT is the same as in Figure 1: the centroid of the RT is located at A and the tool tip at A' such that the angle  $\alpha$  corresponds to  $60^\circ$ . The tool tip traces the path A'B' with  $\alpha$  being  $30^\circ$  at B'. The x- and y-components of the centroidal path AB are defined by Equations (3) and (2) respectively, with the correction factor  $\beta$  in Equation (3) that alters the centroidal path in order to obtain the correct side length indicated in Table 1. The rest of the centroidal path is obtained by symmetry such that the coordinate system is rotated clockwise by  $30^\circ$  to generate the adjacent side of the hexagon, at each of the vertices. This is repeated until all 6 sides are generated. A cavity machined thus is shown in Figure 5b.

In general, the generation of each half side of the polygon of  $n$  sides entails a variation of angle  $\alpha$  between  $60^\circ$  and  $[60^\circ - (180^\circ/n)]$ , and a rotation of the coordinate system by  $(180^\circ/n)$  at each of the  $n$  vertices. The correction factor  $\beta$  becomes negative as  $n$  exceeds 5 (see Table 1).

| $n$     | 5     | 6      | 7      | 8      | 9      |
|---------|-------|--------|--------|--------|--------|
| $s/d$   | 1.17  | 1.46   | 1.84   | 2.09   | 2.34   |
| $\beta$ | 0.012 | -0.025 | -0.057 | -0.053 | -0.054 |

Table 1: Geometric parameters for polygons.

## 5 EDM OF NON-REGULAR POLYGONS

The concepts outlined thus far can be applied also to EDM of non-regular polygons. This involves identification of an appropriate RT tool shape and size, and the catenation of several tool centroid loci that will appropriately generate the various straight line segments of the polygon.

The tool shape is determined by the smallest included angle in the polygon. If this angle is greater than or equal to  $120^\circ$ , a RT can be used as such. For angles between  $60^\circ$  and  $120^\circ$ , the RT needs to be modified as in Figure 3 such that the subtended angle corresponds to the smallest included angle in the polygon. Included angles less than  $60^\circ$  are outside the scope of the present work.

Tool sizing and planning of the tool orbit can be approached in several ways, as there is no unique solution to machining a non-regular polygon. Although simple in principle, these tasks are indeed tedious, as the design of the tool path is to be accomplished in conjunction with the determination of tool size. It is hence best computed using an iterative approach based on geometric modelling.

An example of a non-regular cavity along with its tool trajectory (1.8X) and the corresponding machined shape are depicted in Figures 6a and 6b, respectively. The tool used was a modified RT given that the smallest included angle in the polygon considered is  $90^\circ$ .

## 6 CONCLUSIONS

Innovative kinematic schemes and experimental proof of concept for the seemingly impossible task of using rotating tools for sinking polygonal shapes with sharp corners are presented. The curvilinear tools and the tool paths proposed are motivated by the principle of a Reuleaux Triangle.

Application of this technology enhances flushing of the working gap through rotation and translation of the tool, while concurrently maximising the frontal machining area. The geometry of RT tools further presents the prospect of augmenting process performance by external jet flushing, which can render the removal rate to be independent of the machining depth, unlike conventional EDM.

In view of synchronised tool rotation and translation, X/Y axes feed speeds of CNC ram EDM need be improved from current levels in order to realize higher tool rotational speeds and the benefits thereof. The work represents a substantial advance towards exploiting the capabilities of multi-axis CNC ram EDM that have hitherto remained largely untapped.

## 7 ACKNOWLEDGMENT

This research was funded by the Natural Sciences and Engineering Research Council of Canada.

## 8 REFERENCES

- [1] Kunieda, M., Lauwers, B., Rajurkar, K.P., Schumacher, B.M., 2005, Advancing EDM through Fundamental Insight into the Process, Annals of the CIRP, 54/2:599-622.
- [2] Shibayama, T., Kunieda, T., 2006, Diffusion Bonded EDM Electrode with Micro Holes for Jetting Dielectric Liquid, Annals of the CIRP, 55/1:171-174.
- [3] Masuzawa, T., Heuvelman, C.J., 1983, A Self-Flushing Method with Spark Erosion Machining, Annals of the CIRP, 32/1:109-111.
- [4] Levy, G.N., Ferroni, B., 1976, Planetary Spark Erosion Application and Optimization, 16th Machine Tool Design and Research Conference, Manchester, 291-297.
- [5] Staelens, F., Kruth, J.P., 1989, A Computer Integrated Machining Strategy for Planetary EDM, Annals of the CIRP, 38/1:187-190.
- [6] Yu, Z.Y., Rajurkar, K.P., Shen, H., 2002, High Aspect Ratio and Complex Shaped Blind Micro Holes by EDM, Annals of the CIRP, 51/1: 359-362.
- [7] Rajurkar, K.P., Yu, Z.Y., 2000, 3D Micro-EDM using CAD/CAM, Annals of the CIRP, 49/1:127-130.
- [8] Rajurkar, K.P., Zhu, D., 1999, Improvement of Electrochemical Machining by Using Orbital Electrode Movement, Annals of the CIRP, 48/1:139-142.
- [9] Weisstein, E.W., Reuleaux Triangle, Mathworld, mathworld.wolfram.com/ReuleauxTriangle.html